

Observation of Ground Movement with Existing Pile Groups Due to Tunneling in Sand Using Centrifuge Modelling

Ittichai Boonsiri · Jiro Takemura

Received: 30 August 2014 / Accepted: 13 January 2015 / Published online: 22 January 2015
© Springer International Publishing Switzerland 2015

Abstract In developing urban areas, there are unavoidable interactions between existing structures and new construction such as tunnelling through pre-existing pile foundations. An accurate prediction of the ground deformation due to tunnelling is necessary to assess potential damage to those existing structures. Two dimensional tunnelling model tests were carried out to study the movement of both soil surface and subsurface layers of dry Toyoura sand with two pile groups of different length at both sides of the tunnel. The model pile group has four piles with spacing and diameter ratio of 5. The tunnelling process was simulated by reducing the diameter of the model tunnel with initial diameter of 70 mm for various ground loss values at 100g centrifugal acceleration. The induced soil movement and displacement of pile foundation were observed using the particle image velocity technique and displacement transducers. The test cases were conducted at two different tunnel cover depth and diameter ratios ($C/D = 1.5$ and 2.5) and three different horizontal distances between the pile groups and the tunnel. Tunnel machine showed good agreement of soil movements with the results from

real site construction at small ground loss ratios. The cases with the pile group induced larger maximum settlement in the vertical direction than the cases without piles. There was an effect of the pile groups on the ground movement at the location more than five times pile diameter away from the piles in the longitudinal direction.

Keywords Ground movements · Tunnels · Piles group · Centrifuge

List of symbols

| | |
|-------------|--|
| C | Soil cover depth |
| D | Tunnel diameter |
| X_p | Horizontal distance between the centres of the nearest pile and the tunnel |
| R | Radius of tunnel |
| Z_{pe} | Relative vertical distance between pile toe and centre of tunnel |
| PTM | Potentiometer |
| ΔV | Volume of tunnel contraction |
| V_0 | Initial volume of tunnel |
| \emptyset | Model pile diameter |
| t | Wall thickness of model pile |
| L | Pile embedment length |
| E | Young's modulus |
| EI | Bending rigidity |
| EA | Axial rigidity |
| Q_e | Axial force at the pile toe position |
| Q_h | Axial force measuring by load cell |

I. Boonsiri (✉) · J. Takemura
Department of Civil Engineering, Tokyo Institute of Technology, Tokyo, Japan
e-mail: ittichaiboon88@gmail.com;
Boonsiri.i.aa@m.titech.ac.jp

J. Takemura
e-mail: jtakemur@cv.titech.ac.jp

| | |
|--------------|--|
| S_h | Vertical settlement at pile head level |
| S_e | Vertical settlement at pile toe level |
| S | Ground surface settlement |
| S_{max} | Maximum settlement at the tunnel centre line |
| x | Horizontal distance from the tunnel axis |
| v | Soil vertical settlement |
| x_i | Horizontal distance from the tunnel centreline to the inflection point |
| K | Trough width parameter |
| Z_0 | Depth of tunnel centre |
| Z | Depth of soil |
| V_s | Volume of the settlement trough per unit length |
| PMG | Photometer on the ground |
| PIV | Particle image velocity |
| ΔR | Decrement of model tunnel radius |
| δx | Horizontal movement of pile groups |
| S_p | Soil surface settlements of cases with pile groups |
| S_{np} | Soil surface settlements of cases without pile groups |
| $S_{np,max}$ | Maximum soil surface settlements of cases without pile groups |
| ϕ' | Soil friction angle |
| e | Void ratio of soil |
| e_{max} | Maximum void ratio of soil |
| e_{min} | Minimum void ratio of soil |
| D_{50} | Mean particle diameter of soil |
| U_c | Coefficient of uniformity of soil |
| G_s | Specific gravity of soil |
| D_r | Relative density of soil |
| σ_3' | Confining stress of tri-axial test |

1 Introduction

Ground settlements and movements are inevitably caused by the tunnel construction in soft ground and are major concerns especially in urban areas. Therefore, the tunnelling-induced soil movements have been long studied by many researchers, not only ground surface settlement, but also subsurface settlement (Peck 1969; Mair et al. 1993). The potential effects of the ground movement associated in the tunnel construction must be properly considered in the design and construction of tunnel to avoid the adverse effects, i.e. settlement of the road above tunnel and

damage to adjacent structures, such as pile foundations, buildings, buried pipes etc.

From the research works in literature, such as accumulation of field data, numerical and analytical simulations, prediction of ground movement by tunnelling could have been made reasonably well, which makes it possible to assess the risk of building damage (Mair et al. 1996). Although, these numerical studies have produced interesting results, there are still some uncertainties and the validation of the proposed construction methods is required, especially for the effects of many factors such as, types of soil and tunnelling, imposed soil movement or ground loss by tunnelling, types of piles (single and group), and the effects of piles on the soil movements.

Physical modelling, especially centrifuge modelling is a useful tool to investigate these problems with its capability of creating the similar stresses in a small scale model to those of the full scale prototype. This condition is a critical in a model in which most of stresses and their changes caused by weight of soils, e.g. excavation of soil in tunnelling process. With this advantage, centrifuge modelling has been used for studying tunnelling-induced geotechnical problems and various techniques where tunnelling simulators have been developed.

In the early stage of tunnelling study using the centrifuge, rubber bags with air pressure or liquid pressure were mainly used to investigate the stability of tunnel and deformation of soils (Mair 1979; Takemura et al. 1990). Liquid pressure method is more practical because the volume of ground loss could be measured from amount of extracted liquid. Normally, the rubber bag is attached with the pressure gages to measure the pressure around the tunnel perimeter. In initial condition, hydro-static conditions can be assumed prior extraction of liquid. However, there is some uncertainty in the induced tunnel deformation. The tunnel size could be known from the full-size of rubber bag (initial shape) to the rigid core size of the model tunnel (final shape). But, it is ambiguous about how the diameter is deformed during the pressure is reduced.

To control the tunnel perimeter displacement more accurately, mechanical tunnelling simulators were developed in which a tapered inner core is pulled to decrease the diameter of outer tunnel (Bezuijen and Van der Schrier 1994; Katoh et al. 1998). To simulate the more realistic excavation process and investigate

three dimensional effects, a miniature shield machine (Imamura et al. 1996; Nomoto et al. 1999), and an inflight excavator (König 1998) were also developed.

Soil-pile interactions subjected to tunnelling have also been studied by centrifuge models. Single piles with various relative depth of tunnelling in saturated sandy soil were examined using centrifuge model tests (Lee and Chiang 2007). A zone of large settlements above the tunnel of dense sand layer has been identified by Jacobsz et al. (2004). The results also pointed out the effect of tunnelling on adjacent single pile by centrifuge model. The above mentioned research provided important information about the mechanics of piles subjected to tunnelling-induced soil movements. However, the effect of existing structures for ground movements had very few case records, especially in the case of pile group foundations. The shape of profile settlements may have been altered caused by surrounding buildings. Therefore, a series of centrifuge model tests were carried out to scrutinize the tunnelling-induced soil movement and the effects of pile groups on the soil movement in this study.

2 Centrifuge Model Tests

2.1 Model Setup

The geotechnical centrifuge used in the tests is the Tokyo Tech Mark III Centrifuge, which was installed at Soil Mechanics Laboratory at Tokyo Institute of Technology in 1995. The facility has been described by Takemura et al. (1999). All the experiments were conducted at an acceleration of 100 g. As a result, dimensions of model were scaled by a factor of 100. Figure 1 shows model setup in terms of model scale. The 70 mm diameter model tunnel was located at the centre of the container with 200 mm vertical distance from the container bottom to the tunnel centre. Pile groups with 220 and 150 mm embedment lengths were placed respectively at the both sides of the model tunnel.

The tunnel cover and diameter ratios (C/D) tested were 1.5 and 2.5. Horizontal distance between the closest pile centre and the tunnel centre (X_p), and relative pile toe depth from the tunnel centre (Z_{pe}) are the parameters in the tests, which are normalized by tunnel radius(R). Three horizontal distances of X_p/R

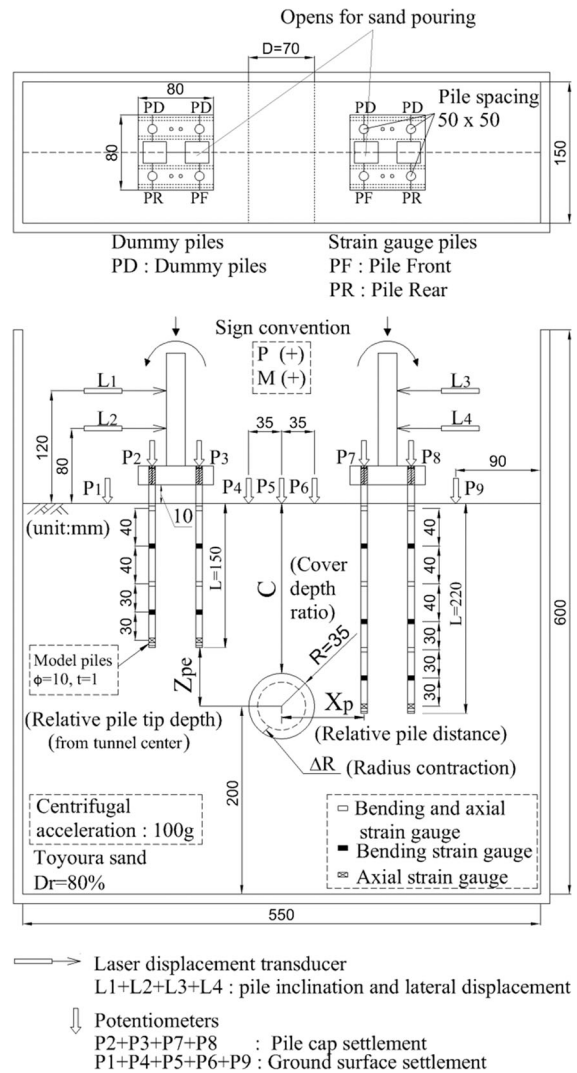


Fig. 1 Layout of test setup

$R = 2.0, 2.5$ and 3.0 were employed. The relative pile toe depth takes on negative values when the pile toe position is shallower than the tunnel centre and positive values when the pile toe position is deeper than the centre, which was varied with Z_{pe}/R from -1.72 to 2.28 .

2.2 Shield Tunnel Model

In this study, a two dimensional mechanical type shield tunnelling machine was employed, which can impose a clear boundary condition at tunnel perimeter, namely, the co-axial tunnel diameter reduction from small to large ground loss ratios. The tunnel model can

steadily maintain the reduction of contraction from the beginning to the end of tunnelling. This shape of contraction could also simulate the tail void formation process for small ground loss ratio ($\Delta V/V_0 < 2.5\%$) in an actual field construction. However, it might be different from the actual condition for large ground loss ratios which is caused by critical conditions such as large over excavation or even failure of the tunnel lining.

The machine comprised a steel ring and a wedge shaped shaft as shown in Fig. 2. The ring was divided longitudinally into six parts, and covered with a steel sleeve and a rubber membrane. The rubber membranes are divided into outer and inner layers. The outer layer is curled round the circular steel rings and these rings are attached at the holes of front and back of the container. The inner layer which is used to cover the tunnel machine was inserted through the outer layer as illustrated in Fig. 2. The steel sleeve was also divided and attached to each steel ring part. The wedge shaped shafts were connected to a screw jack behind the container, which can move horizontally inward and outward as shown in Fig. 3. The figure illustrated the reduction in tunnel diameter from initial to final condition of the tunnel machine by pulling out the screw jack along the taper angle of the wedge shaped shaft. This process changed the position of the ring in the radial direction. This model tunnel covered with a

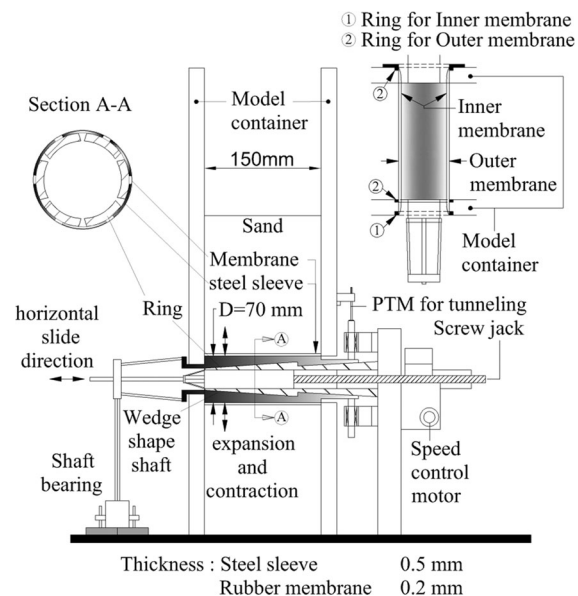


Fig. 2 Shield tunnelling model

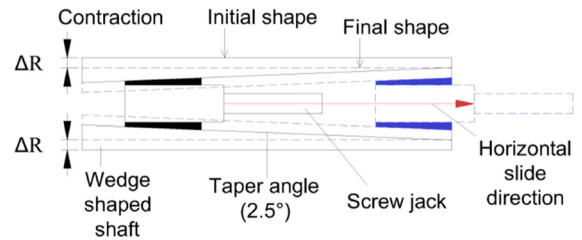


Fig. 3 Simplified mechanism of tunnel deformation

rubber membrane could expand or contract its diameter. The rubber was used for a consistent circular shape transformation of the tunnel when it reduced or increased the diameter. Moreover, this rubber membrane also prevented sand intrusion inside the model tunnel. One potentiometer (PTM) was installed on the shaft which was connected to the screw jack to measure the diameter change of model tunnel during the in-flight excavation. At the same positions in the front and back walls of model container, circular holes were cut into which the shield tunnel model was inserted. The gaps between the tunnel model and the circular holes were filled with silicone material to prevent leakage of the sand.

The ground loss ratio ($\Delta V/V_0$) was adopted as a parameter controlling tunnel-induced ground displacement (Loganathan and Poulos 1998). ΔV is the volume of the gap formed around the tunnel per unit tunnel length, namely reduction of tunnel cross sectional area. V_0 is the initial volume of tunnel, in other words, the initial tunnel cross sectional area. The initial diameter of the shield model was 70 mm (7 m in prototype scale) which could reduce to minimum value of 60 mm (6 m in prototype scale), which can introduce $\Delta V/V_0$ up to 26 %. However, due to the discontinuous behaviour of the machine at a large contraction portion, the ground loss ratio was varied from 0 to 15 %. This range of $\Delta V/V_0$ enabled the behaviour ranging from working condition to critical conditions close to failure to be observed. The diametrical rate of contraction was controlled from 0.1 to 1.3 mm/s. In the tests, around 200 s was taken to complete the reduction of tunnel diameter.

2.3 Model Piles and Pile Cap

An acrylic hollow cylinder with Young's modulus (E) of 3.2 GPa was selected to make model piles of 10 mm diameter (\varnothing) and 1 mm (t) wall thickness with

embedment length (L) of respectively 220 and 150 mm as described in Fig. 1. The acrylic pile is quite flexible and has large yield strain which is possible to assume linear relation during induced high magnitude of ground loss in the tunnelling process. One of advantage for this pile material is repeatability. However, one of limitation of the acrylic pile is small bending and axial rigidity as indicated in Table 1. The coefficient of friction between dry sand and acrylic materials is approximately around 0.25–0.30. The coefficient of friction could be measured by pushing a block of acrylic on the flat and compact dry sand in horizontal direction. The load of pushing block was measured by load cell.

Inside the hollow acrylic pile, strain gauges were placed to measure axial and bending strain. Brass plugs were inserted at the toe of model piles. The pile caps were made from 20 mm thick stainless steel plate and were connected rigidly to the vertical piles positioned at a centre-to-centre spacing of 50 mm. Considering the symmetrical arrangement of the pile group models, one pile group consisted of two strain gauged piles in the first row and two dummy piles in the second row as described in Figs. 1 and 4. Two 2×2 pile groups with longer and shorter piles are installed on either side of the tunnel in the dry sand. Acrylic or aluminium plate was fixed on top of the pile cap to add an extra-weight to the pile group. Total masses of 760 and 1,040 g were applied on the short pile group. As a result, one pile model carried a distributed load equal to 1,900 and 2,600 kN at the prototype scale respectively. While 1,040 and 2,030 g masses were added to the long pile group to have distributed load equal to 2,600 and 5,075 kN at the prototype scale per pile respectively. A summary of applied load per pile is shown in Table 3.

Vertical load tests were conducted to measure the bearing capacity of the model piles which were prepared in a container without a model tunnel with the same relative density of the sand for the tunnelling model ($D_r = 80\%$). Short and long pile groups which were gradually loaded by a mechanical jack and pile load and cap settlements were measured by a load cell and potentiometers at prototype scale. Vertical settlements of the pile which, were measured at the pile head (S_h) and pile toe (S_e), were plotted against axial force measured by the load cell (Q_h) and the strain gauges at the pile toe position (Q_e) as shown in Fig. 5. Terzaghi (1942) proposed that the ultimate bearing capacity of piles can be acquired from pile-load settlements curve at 10 % of the pile diameter settlements. However, in this study, the acrylic pile behaved flexibly due to its relatively low stiffness. Therefore, vertical settlement of the pile toe was

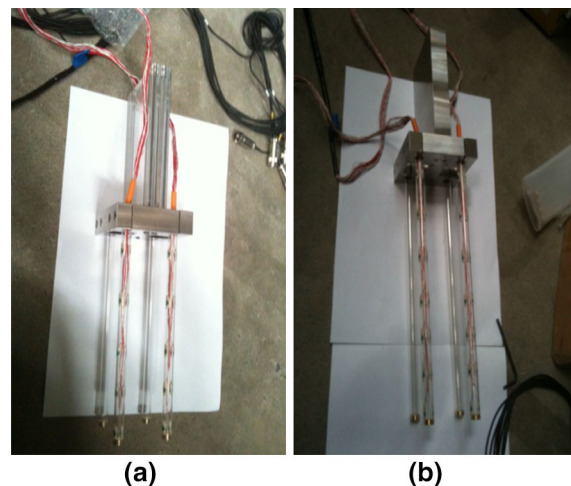


Fig. 4 Assembly of pile group models a short piles; b long piles

Table 1 Pile properties in model scale and prototype scale

| Properties | Model | Prototype | Prototype | Prototype |
|----------------------------|----------------------|------------------------|------------------------------|-----------------------|
| Material | Acrylic pile | Acrylic pile | Concrete pile | Steel pipe |
| Diameter (\varnothing) | 10 mm | 1.0 m | 1.0 m | 42 in. (1.05 m) |
| Thickness (t) | 1 mm | 0.1 m | Solid | 0.5 in. (0.0125 m) |
| Young's modulus (E) | 3.2 GPa | 3.2 GPa | 20–28 GPa | 200 GPa |
| Embedment depth (L) | 150 mm | 15 m | 15 m | 15 m |
| | 220 mm | 22 m | 22 m | 22 m |
| Bending rigidity (EI) | 0.93 Nm ² | 0.093 GNm ² | (0.98–1.37) GNm ² | 1.09 GNm ² |
| Axial rigidity (EA) | 0.09 MN | 0.9 GN | (15.7–21.9) GN | 8.15 GN |

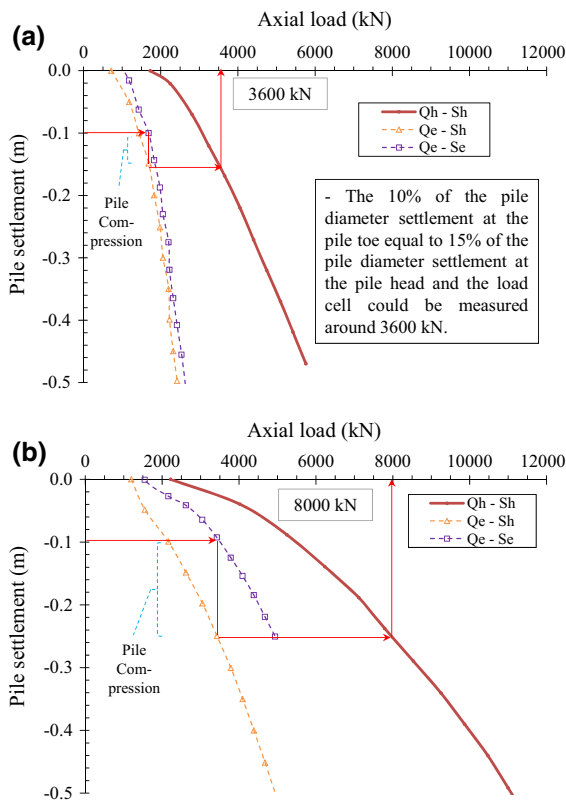


Fig. 5 **a** Pile load test of short pile group ($L = 14$ m); **b** pile load test of long pile group ($L = 21$ m)

estimated by subtracting the pile compression from the pile head settlement. Pile compressions along the piles were calculated from average axial strains of two consecutive points of strain gauges and multiplied it by the distance between those consecutive points. Considering the compression of the pile, the pile bearing capacity can be determined from the pile head load at 10 % pile diameter settlements at the pile toe position as shown in Fig. 5. Pile bearing capacity were found to be approximately around 3,600 and 8,000 kN for short and long model pile respectively.

3 Test Procedures and Conditions

3.1 Model Preparation

Models were placed and tested in an aluminium container with an internal plan area of 150 mm width and 550 mm length and an internal height of 600 mm (Fig. 1). The front wall of the container was made of

acrylic plate, through which the ground movement could be observed. As the tunnel model contracted uniformly in the radial direction, the soil in the model displaced two dimensionally for the case without piles.

Two assembled pile groups were suspended on either side of the tunnel at the predetermined vertical and horizontal locations at equal horizontal distances from the tunnel axis for each case. Dry Toyoura sand (Table 2) was then pluviated by a hopper with a constant falling height and flow rate. The miniature hopper was connected with small diameter tube to make certain that sand could fill the small space underneath the pile cap. The hopper was calibrated at vertical and incline directions to make sure of the target density. Two openings at the pile cap (see also Fig. 1) were provided for inserting the tube to place the sand between the pile models. The sand was poured by layers in 20 mm thickness each until it reached the designed depth. Drained tri-axial compression tests using Toyoura sand and various relative densities were carried out by Fukushima and Tatsuoka (1984), Tatsuoka et al. (1986). They found that the internal friction angle (ϕ') decreased with the void ratio (e). As a result, the relation between the confining stress (σ_3') and internal friction (ϕ') at the void ratio around 0.68–0.70 ($D_r \approx 80\%$) was proposed. In addition, they also pointed out that although the internal friction angle (ϕ') decreased with increasing of the confining stress (σ_3'), the internal friction angle (ϕ') was almost constant when the confining stress (σ_3') was <50 kPa. Therefore, by using there correlation, the internal friction angle (ϕ') of dry Toyoura sand was approximated to be 40° .

After the sand preparation, the box was mounted on the centrifuge platform. Pairs of potentiometers and laser displacement transducers were placed to measure the displacement (horizontal and vertical movements, and inclination) of each pile cap. Potentiometers were also placed on the sand surface to measure the surface settlements as shown in Figs. 1 and 6. A digital camera

Table 2 Dry Toyoura sand properties

| | |
|-------------------------------------|------------|
| Specific gravity (G_s) | 2.65 |
| Mean particle diameter (D_{50}) | 0.19 |
| Coefficient of uniformity (U_c) | 1.62 |
| Maximum void ratio (e_{max}) | 0.973 |
| Minimum void ratio (e_{min}) | 0.609 |
| Soil friction angle (ϕ') | 40° |

(Canon Power-Shot G7) was fixed at the front of the box to capture the images of soil movements through the front window (Fig. 6). This camera can be operated and monitored via a wireless connection into the control room during the centrifuge operation. The brightness and spatial variation of ground model texture affects the result of displacement (White et al. 2003). Rows of LED lights were installed on the upper and lower position of the front window to enhance image quality.

3.2 Test Conditions and Tunnelling Tests

Three series of model tests were conducted. Test conditions are shown in the Table 3. In test series A, tunnelling processes were studied without pile installation for the models of tunnel cover and diameter ratio (C/D) equal to 1.5 and 2.5, where C is the distance between the ground surface and the tunnel crown, and D is the initial tunnel diameter (70 mm). These test results will be used as a basic behaviour of induced ground movements in contrast to those with existing piles. In test series B, both short and long piles were embedded with $C/D = 2.5$. The horizontal distance between the piles and tunnel was varied ($X_p = 2.0, 2.5,$ and $3 R$). The horizontal distances

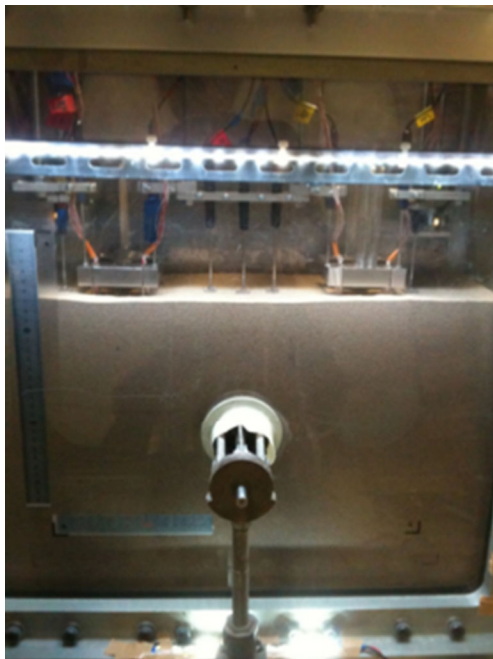


Fig. 6 Front view of model preparation

were measured between the centre of the tunnel and the closest pile of the pile group as illustrated in the Fig. 1. In test series B(1), the distributed loads per pile from the weight and the pile cap were 2,600 and 5,075 kN for short and long pile groups respectively at the prototype scale. In test series B(2), the distributed load were reduced to 1,900 and 2,600 kN for both short and long pile groups respectively. In test series C, the distributed loads were the same as in test series B(2) except the tunnel cover and diameter ratio ($C/D = 1.5$). The relative pile toe depth to the tunnel (Z_{pe}) was varied with different C/D s and pile embedment lengths. Positive and negative sign conventions of Z_{pe} depend on the positions between the pile toes and the tunnel model. Positive signs mean the pile toes are deeper than the tunnel model and negative signs when the pile toes are shallower than the tunnel model. In Table 3, test conditions of eleven tests are given by normalized values, C/D , X_p/R and Z_{pe}/R . In the case $X_p/R = 3.0$, the distance from the container side wall and the rear side piles was a minimum of 120 mm (twelve times pile diameters) that is considered adequate to minimize the boundary effects (Lee and Chiang 2007).

Having completed the instrumentation of the model, the centrifuge model was accelerated until it reached 100g. After confirming the steady condition in all measurements, the tunnelling test was started reducing the diameter from 70 to 64.5 mm for simulating the tunnelling process two dimensionally. The average time for the tunnelling process was about 200 s. During the tunnelling process, the digital camera captured the image of the front side of container every 20 s. The radial contraction of the tunnel was measured by potentiometer, which was converted to the imposed ground loss ratio ($\Delta V/V_0$).

4 Test Results

4.1 Particle Image Velocimetry (PIV) Technique

GeoPIV which uses particle image velocimetry (PIV) in a MatLab program (White and Take 2003) was employed to observe the displacement of model ground. The digital images were captured during the reduction of tunnel diameter and were used in the GeoPIV program. The soil layers above the model

Table 3 Test Conditions and results

| Test series | Case | C/D | X_p/R | D_r (%) | Short pile | | | Long pile | | | x_i/R | |
|-------------|---------|-----|---------|-----------|------------|-----------------------|---------------------------------|------------|-----------------------|---------------------------------|----------------|------|
| | | | | | Z_{pe}/R | Mass ^a (g) | Load per pile ^b (KN) | Z_{pe}/R | Mass ^a (g) | Load per pile ^b (KN) | $\Delta V/V_0$ | |
| | | | | | | | | | | | 2 % | 15 % |
| A | Case 0D | 2.5 | – | 80 % | – | – | – | – | – | – | 2.6 | 2.2 |
| | Case 0S | 1.5 | – | – | – | – | – | – | – | – | 1.8 | 1.5 |
| B(1) | Case 1D | 2.5 | 2.0 | – | –1.72 | 1,040 | 2,600 | 0.28 | 2,030 | 5,075 | 3.3 | 2.6 |
| | Case 2D | 2.5 | 2.5 | – | –1.72 | 1,040 | 2,600 | 0.28 | 2,030 | 5,075 | 3.2 | 2.5 |
| | Case 3D | 2.5 | 3.0 | – | –1.72 | 1,040 | 2,600 | 0.28 | 2,030 | 5,075 | 2.9 | 2.2 |
| B(2) | Case 4D | 2.5 | 2.0 | – | –1.72 | 760 | 1,900 | 0.28 | 1,040 | 2,600 | 3.0 | 2.4 |
| | Case 5D | 2.5 | 2.5 | – | –1.72 | 760 | 1,900 | 0.28 | 1,040 | 2,600 | 2.9 | 2.4 |
| | Case 6D | 2.5 | 3.0 | – | –1.72 | 760 | 1,900 | 0.28 | 1,040 | 2,600 | 2.7 | 2.3 |
| C | Case 1S | 1.5 | 2.0 | – | 0.28 | 760 | 1,900 | 2.28 | 1,040 | 2,600 | 2.0 | 1.7 |
| | Case 2S | 1.5 | 2.5 | – | 0.28 | 760 | 1,900 | 2.28 | 1,040 | 2,600 | 1.9 | 1.6 |
| | Case 3S | 1.5 | 3.0 | – | 0.28 | 760 | 1,900 | 2.28 | 1,040 | 2,600 | 1.8 | 1.6 |

D = 7.0 m, R = 3.5 m

^a Model, ^b prototype

tunnel were divided into patches in the GeoPIV software (Fig. 7a). The resolution from the digital camera used (Canon Power-Shot G7) was 180 pixels per 25.4 mm. This range converts to 0.14 mm/pixels in object scale displacement in the model. The patch size which was used in this analysis was 128 pixels or 18 mm. As a result, spacing between displacement vectors are equal to 18 mm on both horizontally and vertically directions. In addition, the search zone length area between sequence images was imposed to 12 pixels. The first subsurface layer was at 12 mm depth from the ground surface and the deepest layer was at 138 mm depth and 84 mm depth for C/D ratio of 2.5 and 1.5 respectively.

The displaced vectors (Fig. 7b) show a trend corresponding to the normal distribution profile, where the highest movements are concentrated at the centre-line above the tunnel model. The movements decrease with distance from the tunnel axis.

4.2 The Accuracy of PIV Technique

In order to prove the accuracy of PIV measurements, the measured data by PIV were compared with those by potentiometers for the tunnel models without the pile groups (Cases 0D and 0S), in which pure two-dimensional deformation could be assumed.

Ground surface settlements measured by PIV at the locations of the potentiometers (Fig. 8) and those measured by potentiometers are plotted against ground loss ratio $\Delta V/V_0$ in Fig. 9. In the legend of the figure, the digits after PMG and PIV indicate the horizontal coordinate of the measurement points, that is, the distance from the tunnel centre line in a unit of metre. For small to medium ground loss ratios (<7–10 % $\Delta V/V_0$), the graphs show symmetrical settlement for the left and right sides of tunnel. However, they show slightly uneven settlements at large ground loss ratios.

The magnitude of settlements obtain by potentiometers were slightly larger than the PIV results, especially for large ground loss ratios in Case 0S (C/D = 1.5). This might come from the friction between the sand and the window surface of container. However, the difference is small and almost negligible for relatively small ground loss ratios, less than 7–10 %. From this fact, it can be said that the accuracy of PIV results can be considered to be acceptable. In addition, it is also inferred that the displacements measured at the front portion of the model by PIV can be considered equal to the displacements of the central portion of the model without the pile groups. In addition, the local effects of existing pile foundations could be observed when comparing the soil surface

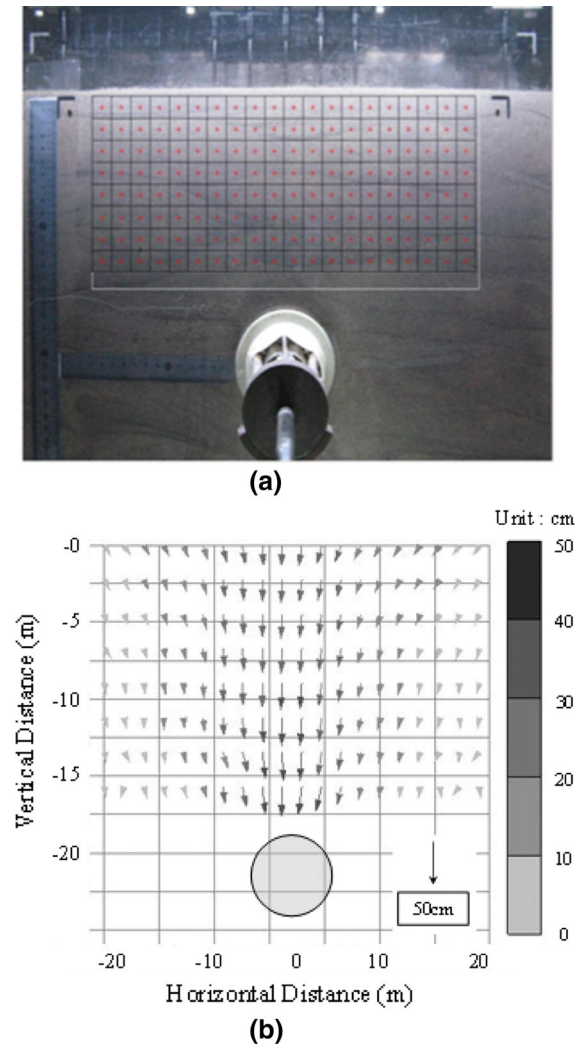


Fig. 7 **a** Divided mesh of sequence images; **b** displacement vectors of subsurface layers from PIV at $\Delta V/V_0 = 14.0\text{--}14.5\%$

settlement between the centre of the model central container and the front of the screen.

4.3 Ground Movements by Tunnelling

The ground movements caused by tunnel construction need to be evaluated for safety issue implications on adjacent structures. From a substantial amount of data in case records (Peck 1969; Schmidt 1969; O’Reilly and New 1982; Mair and Taylor 1997), the shapes of soil surface settlement trough developing during tunnel excavation are well described by a normal distribution curve as

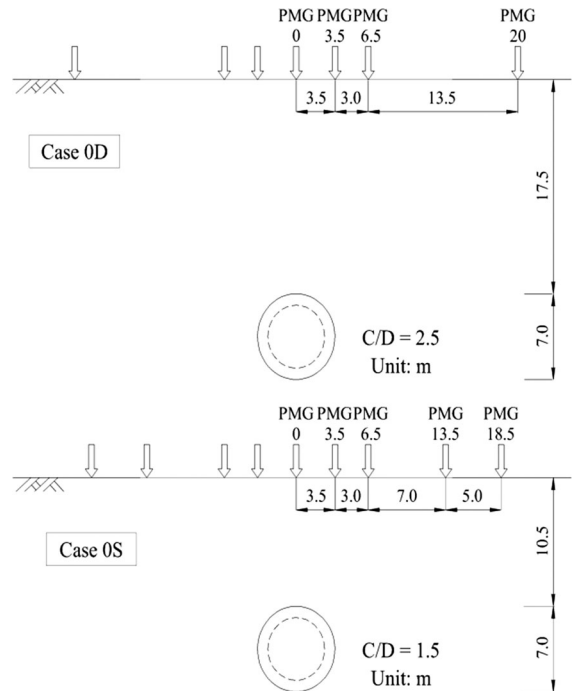


Fig. 8 PTM positions of Case 0D and Case 0S

$$S(x) = S_{max} \exp\left(\frac{-x^2}{2x_i^2}\right) \tag{1}$$

where $S(x)$ is the settlement at a horizontal location x from tunnel axis, S_{max} is the maximum settlement at the tunnel centre line, $x = 0$, and x_i is the transverse distance from the tunnel centreline to the inflection point of the curve.

The main features of the normal distributed curve and the parameters are shown in Fig. 10. The settlement at the inflection point is about $0.606S_{max}$ and the half-width of the settlement trough is approximately about $2.5x_i$.

The settlement troughs at different depths of the models without pile groups are compared with those with pile groups located at $X_p = 2R$ for small and large $\Delta V/V_0$ ratios in Fig. 11. In the figures the settlements are normalized by the decrement of tunnel radius (ΔR) and horizontal distance x is normalized by tunnel radius. A wedge-shaped boundary region has been proposed for large induced settlements due to tunnelling (Loganathan and Poulos 1998). In addition, a zone of influence with large induced soil movements is also reported by Kaalberg et al. (1999), Jacobsz et al. (2004), Selemetas et al. (2006). At the potentiometers

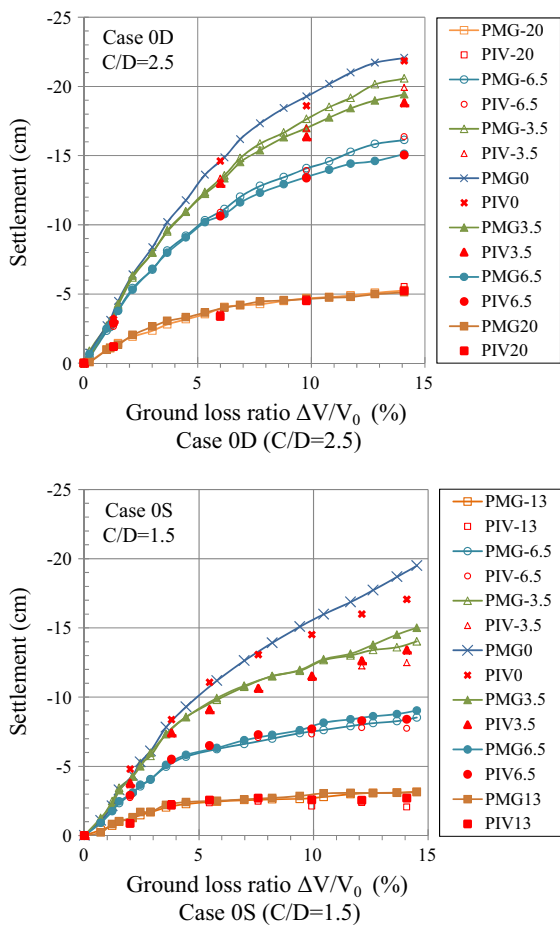


Fig. 9 Comparisons of surface settlements measured by PTM and PIV of Case 0D and Case 0S

far from the tunnel, the settlements reduced due to being outside the wedge-shaped boundary and zone of influence. The potentiometers within this area will suffer from large vertical settlement.

For cases with $C/D = 1.5$, negligible settlement is confirmed at large normalized horizontal distance ($x/R > 5$, $x/R < -5$), while for $C/D = 2.5$, settlement is still observed in those positions as shown in Fig. 11. This indicates that the cover and depth ratio has an effect on the chimney-shape mechanism (Cording 1991; Potts 1976), where large displacements occur in the area directly above the tunnel. The chimney-like mechanism is more noticeable for the cases with $C/D = 1.5$ than the cases with $C/D = 2.5$.

Deep layers show narrower troughs than the shallower layers near the surface. The results also support that trough width has been found to vary with

the depth of interest (O'Reilly and New 1982; Hergarden et al. 1996; Mair and Taylor 1997). The shapes of the trough were symmetrical. However, in the models with the pile groups, the width of the troughs tended to increase. These results will lead to different inflection points for the subsurface settlement troughs for models with and without pile groups

From the previous observation, O'Reilly and New (1982) showed that the trough width parameter (x_i) is an approximately linear function of tunnel depth (Z_0) as shown below:

$$x_i = KZ_0 \quad (2)$$

where K is the empirical constant, called trough width parameter, that can be taken as an average value of 0.4 for stiff clay to 0.7 for soft and silty clay, and 0.2–0.3 for granular material, regardless of tunnel size and tunnelling method.

For subsurface settlements at depth Z , it is also assumed that the shapes of subsurface settlement profiles can be represented by a Gaussian distribution curve, Eq. (1). However, Z_0 in Eq. (2) is replaced by $(Z_0 - Z)$ and K value varies with depth. It has been found that troughs in the subsurface are narrower and steeper than that at the surface (Attewell and Farmer 1974; Barratt and Tyler 1976; Glossop 1978; Mair 1979; Mair et al. 1993).

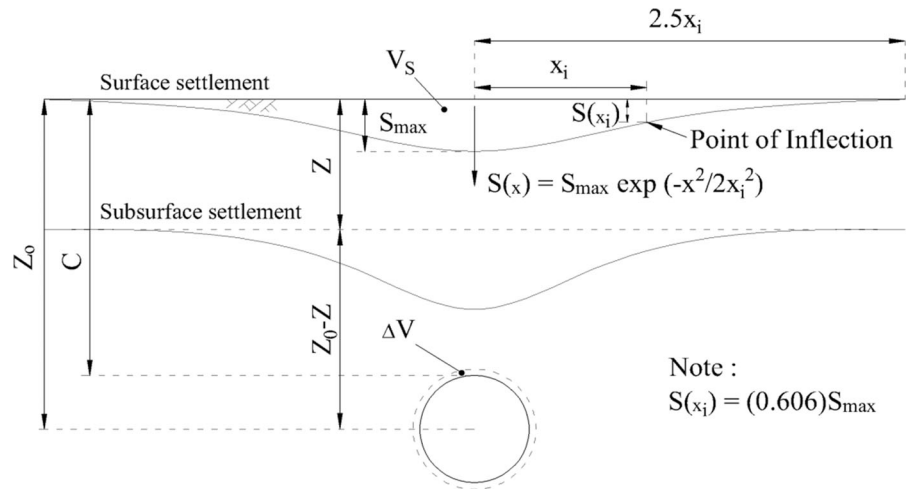
For tunnels in sand, Moh et al. (1996) proposed the equation of a distributed K -value obtained from field data. The effect of tunnel diameter (D) and an empirical constant value (m) is included as indicated in the following equation

$$K = \frac{\left(\frac{D}{2}\right) \left(\frac{Z_0}{D}\right)^{0.8} \left(\frac{Z_0 - Z}{Z_0}\right)^m}{Z_0 - Z} \quad (3)$$

The empirical value of m is equal to 0.4 and 0.8 for sand and clay respectively.

Marshall et al. (2012) conducted centrifuge tests in dry sand with a brass cylinder as a model tunnel. The brass cylinder was covered with a latex membrane and the annulus between the brass cylinder and the latex membrane is filled with water. The brass cylinder position was assembled eccentrically near the bottom of the tunnel. Marshall et al. (2012) found that the Gaussian curve could not provide a good fit to the settlement data (i.e. Dyer et al. 1996) but that curves with three degrees of freedom, i.e. modified Gaussian curve by Vorster et al. 2005; and yield–density curve

Fig. 10 Parameters and settlement profile described by normal distribution curve



(Shapes of settlement troughs depend on ground yielding around the tunnel) by Celestino et al. 2000 can provide a good fit to the settlement data. In addition, it is difficult to compare these curves with other published data which use standard parameters of K and x_i . Therefore, Marshall et al. (2012) developed three degrees of freedom curves based on three points on the Gaussian curve (i.e. S_{max} , $0.606S_{max}$ and $0.303S_{max}$) from centrifuge test results as shown in Eq. (4). The curve combined the effect of depth, C/D and ground loss ratio.

$$K^* = \frac{K_s^* - 0.436\left(\frac{Z}{Z_0}\right)}{1 - \frac{Z}{Z_0}} \tag{4}$$

$$K_s^* = 0.440 + 0.055\left(\frac{C}{D}\right) - 0.041\left(\frac{\Delta V}{V_0}\right)$$

where K^* is equal to K of previous published data based on the fit of a Gaussian curve, K_s^* is K^* at soil surface. In addition, the coefficients of K_s^* come from the plot of K_s^* and $\Delta V/V_0$, and K_s^* and C/D .

4.4 Comparison of K Value

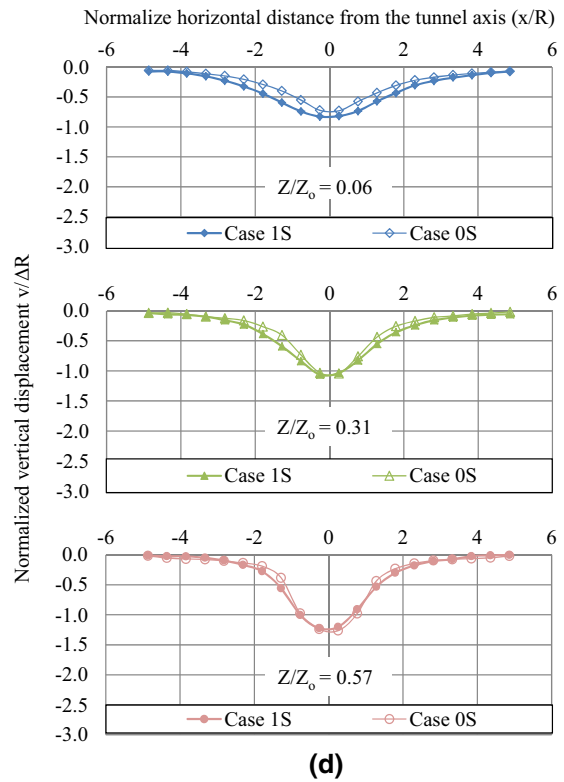
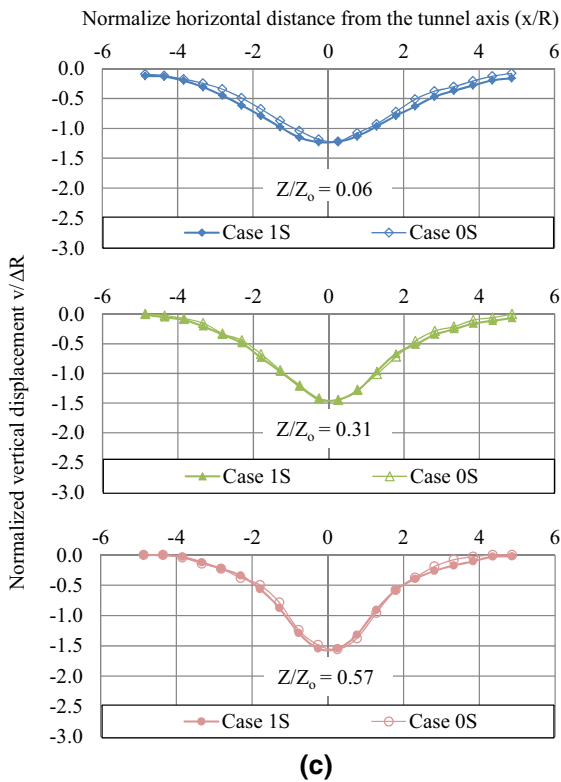
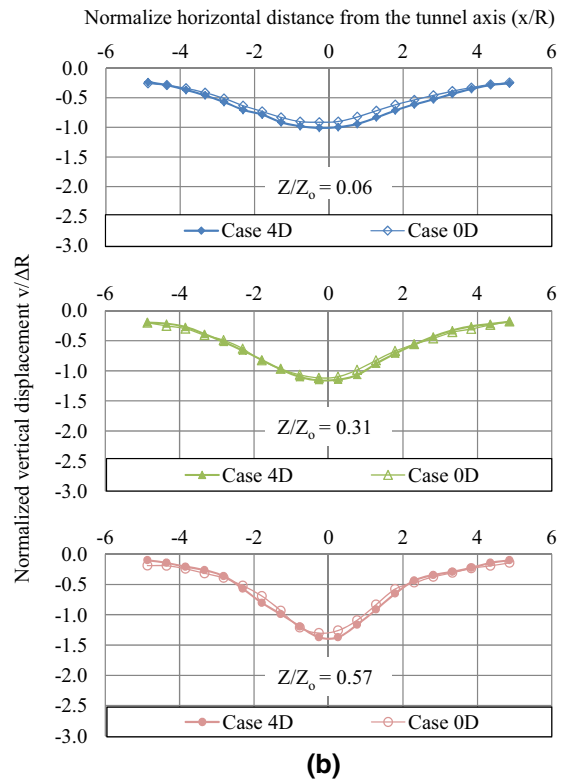
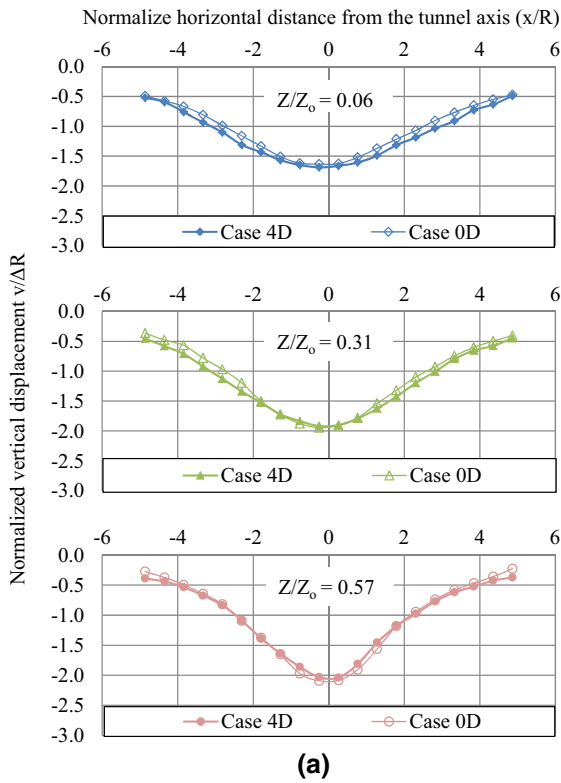
Many previous researches proposed trough width parameters K defined by Eqs. (3) and (4) as a function of the relative depth (Z/Z_0). In this study, the parameters were obtained from the average horizontal distance of the inflection points (x_i) of the trough curve, which were estimated at $S = 0.606S_{max}$ at the right and left sides. In Fig. 12, K values obtained from

PIV results are plotted against normalized depth Z/Z_0 for small and large ground loss ratios. In the figure, the normalized relations reported by Dyer et al. (1996), Moh et al. (1996), and Marshall et al. (2012) are also given.

Moh et al. (1996) derived a correlated relation between K and depth [Eq. (3)] from the data observed during the construction of the Taipei Rapid Transit Systems (TRTS) using a 6 m diameter earth pressure balancing shield machine with tunnel cover depth of about 15 m in sandy soil. The cover to depth ratio is equal to 2.5, which is very similar to the experimental model.

Dyer et al. (1996) analysed the monitored settlements in pipe-jacking/tunnelling works for a sewer pipe with 1.2 m diameter in a stratum of loose to moderately dense glacial sands at Well'ith Lane, Rochdale.

As shown in Fig. 12, both tunnel models with $C/D = 1.5$ and 2.5 displayed similar trends, that is, K values increasing with the depth. Result of Case 0S and Case 0D ($C/D = 1.5$ and 2.5 , without pile groups) for small ground loss ratio ($\Delta V/V_0 < 2.5\%$) showed good agreement with that estimated data from Moh et al. (1996) which was obtained from sandy ground layers for relatively small $\Delta V/V_0$ at an actual construction site. The results imply that tunnel boring machine can simulate tunnelling process in an actual field condition at small ground loss ratios. In addition, in the cases with pile groups (Case 1D, Case 3D, Case 4D and Case 6D for $C/D = 2.5$ and Case 1S and Case 3S for $C/D = 1.5$), K values tended to increase as



◀ **Fig. 11** Subsoil vertical displacement profiles for the case with and without pile groups measured by PIV. **a** Case 0D and 4D ($C/D = 2.5, X_p/R = 2.0$), $\Delta V/V_0 = 2.0\text{--}2.5\%$. **b** Case 0D and 4D ($C/D = 2.5, X_p/R = 2.0$), $\Delta V/V_0 = 14.0\text{--}14.5\%$. **c** Case 0S and 1S ($C/D = 1.5, X_p/R = 2.0$), $\Delta V/V_0 = 2.0\text{--}2.5\%$. **d** Case 0S and 1S ($C/D = 1.5, X_p/R = 2.0$), $\Delta V/V_0 = 14.0\text{--}14.5\%$

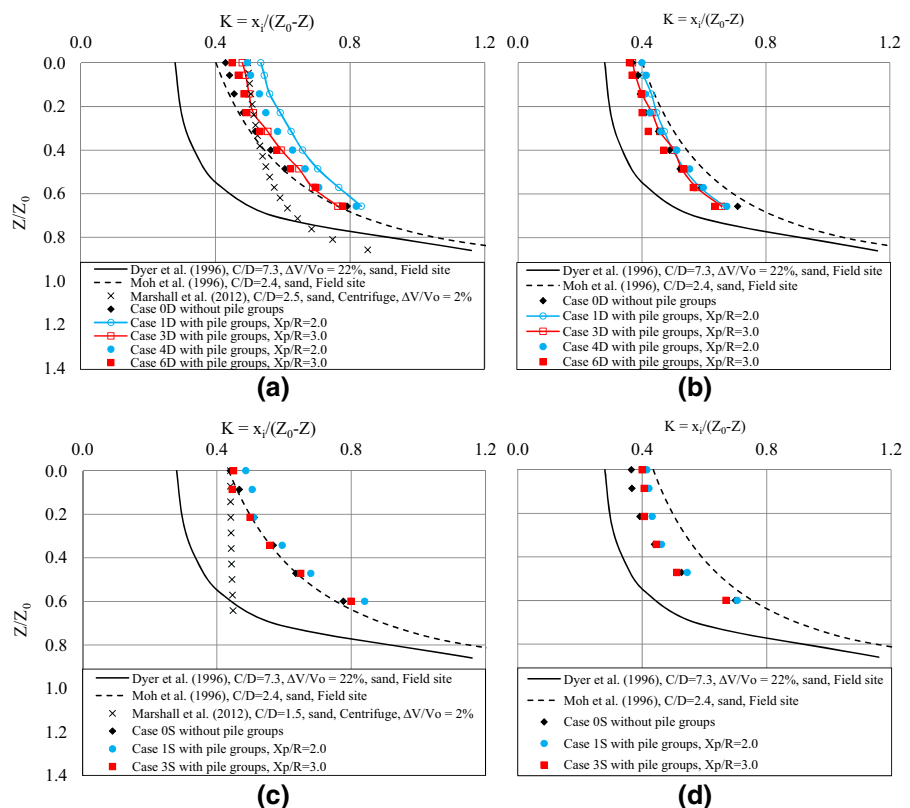
the pile groups position got close to the tunnel. Nevertheless, the observed trend of K value change from small to large ground loss ratio compares well with the difference between Moh et al. (1996) and Dyer et al. (1996). However, the observed K values at large ground loss ratios are larger than those by Dyer et al. (1996), which could be attributed to the difference in the movement of the tunnel perimeter between the test condition and the actual site condition for large ground loss ratio as pointed out in Sect. 2.2. In addition, in Fig. 12, the distributed K values obtained from Eq. (4) (Marshall et al. 2012) are also illustrated in the figure. The curves were estimated by using a ground loss ratio ($\Delta V/V_0$) equal to 2 % and a cover to depth ratio (C/D) equal to 2.5 (Fig. 12a), and

1.5 (Fig. 12c) respectively. The proposed results from Marshall et al. (2012) showed an underestimated distribution of K values when compared to the results from this study and Moh et al. (1996). It may come from the different boundary conditions of the tunnel model. The Marshall et al. (2012) model provided a larger liquid-filled annulus space at the crown than at the invert positions. From curves plotted by Marshall et al. (2012), the increments of K values along the soil depth became gradually smaller in magnitude with increasing ground loss ratios, especially at small cover to depth ratios ($C/D = 1.5$, Fig. 12c).

These results can be summarized that in cases of large ground loss values, the shape of normalized trough settlements (Fig. 11) becomes steeper at the central portion than in the cases with small ground loss values. Hergarden et al. (1996), Jacobsz (2002), Vorster (2005) also concluded that trough width reduces with increasing ground loss ratio.

In addition, the values of x_i were found to reduce with depth and the reductions were almost linear for the cases with $C/D = 1.5$ (Case 0S) and 2.5 (Case 0D)

Fig. 12 Variation of K with depth for subsurface settlement profiles. **a** $C/D = 2.5, \Delta V/V_0 = 2.0\text{--}2.5\%$. **b** $C/D = 2.5, \Delta V/V_0 = 14.0\text{--}14.5\%$. **c** $C/D = 1.5, \Delta V/V_0 = 2.0\text{--}2.5\%$. **d** $C/D = 1.5, \Delta V/V_0 = 14.0\text{--}14.5\%$



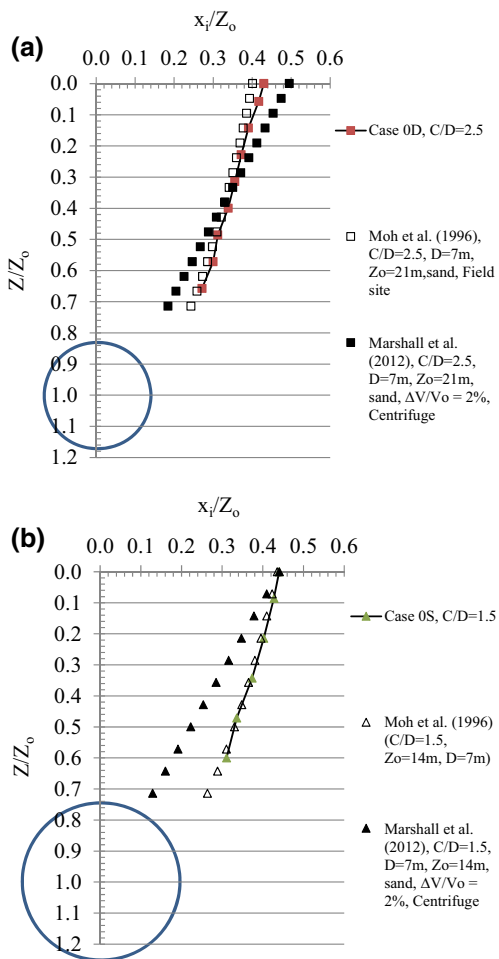


Fig. 13 Distribution of x_i along the relative soil depth at $\Delta V/V_0 = 2\text{--}2.5\%$ for: **a** Case 0D and **b** Case 0S

as shown in Fig. 13. In the figure, the values of x_i which were calculated by Eq. (3) (Moh et al. 1996) and Eq. (4) (Marshall et al., 2012) as well as values from this study were plotted. The test results showed similar trends of a linear reduction of x_i with depth than the results proposed by Moh et al. (1996) and the trend of x_i reducing towards the tunnel spring line for the cases with $C/D = 2.5$ (Fig. 13a) and cases with $C/D = 1.5$ (Fig. 13b). In addition, the results proposed by Marshall et al. (2012) showed that the trend of x_i reduction tended to reduce toward the centre of the tunnel. The different trends could be attributed to the difference of boundary conditions of different tunnel models. The soil movement was concentrated at the tunnel crown for the tunnel model with a large annulus space at the tunnel crown (Marshall et al. 2012).

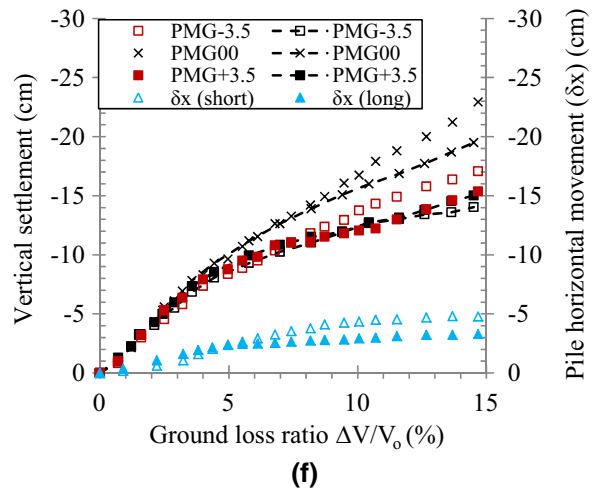
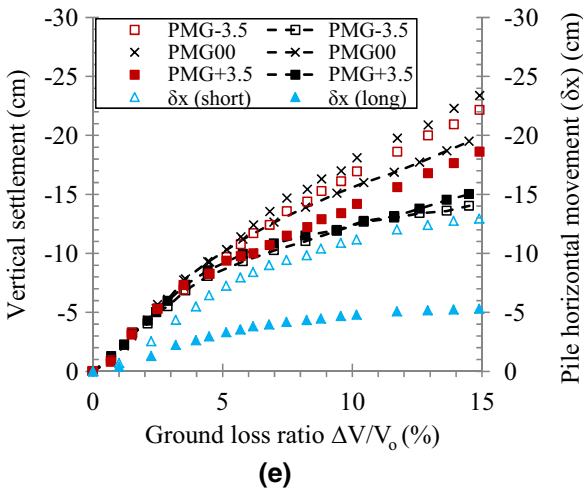
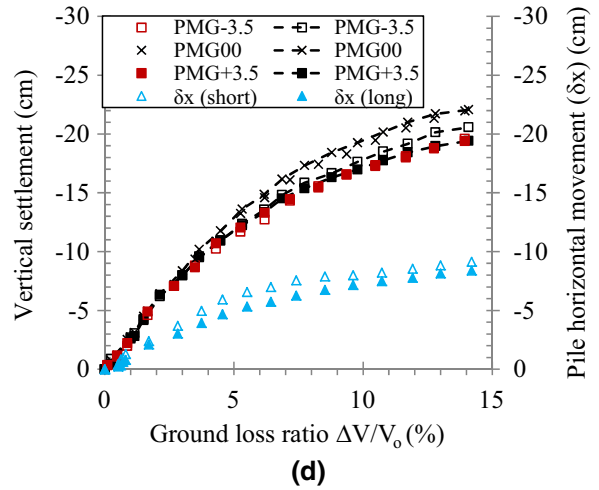
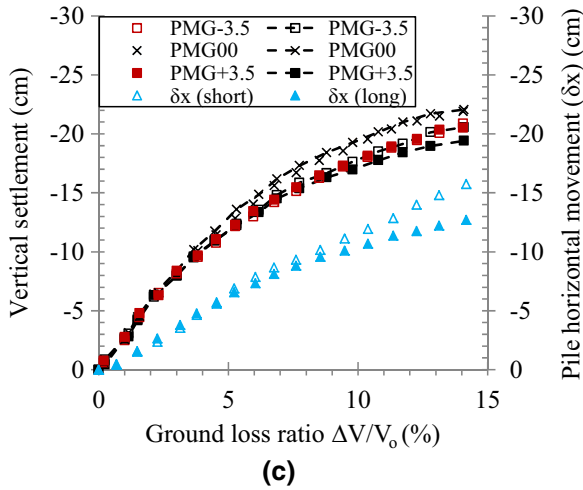
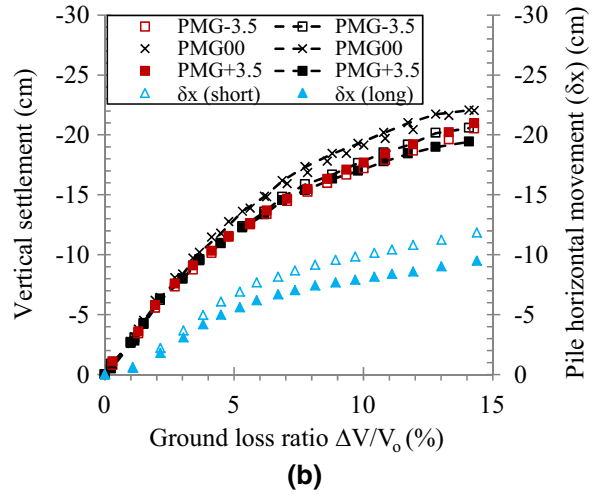
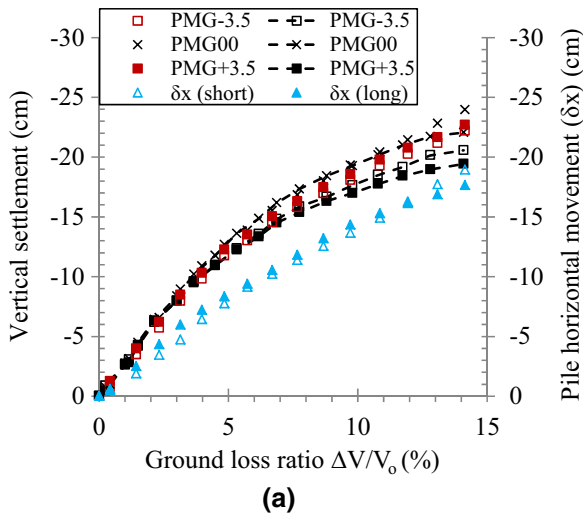
Fig. 14 Soil surface settlements and horizontal displacements of pile cap against ground loss ratio: potentiometer measurements. **a** Case 1D ($C/D = 2.5$, $X_p/R = 2.0$). $Z_{pe}/R = -1.72$ (short); 0.28 (long). **b** Case 3D ($C/D = 2.5$, $X_p/R = 3.0$). $Z_{pe}/R = -1.72$ (short); 0.28 (long). **c** Case 4D ($C/D = 2.5$, $X_p/R = 2.0$). $Z_{pe}/R = -1.72$ (short); 0.28 (long). **d** Case 6D ($C/D = 2.5$, $X_p/R = 3.0$). $Z_{pe}/R = -1.72$ (short); 0.28 (long). **e** Case 1S ($C/D = 1.5$, $X_p/R = 2.0$). $Z_{pe}/R = 0.28$ (short); 2.28 (long). **f** Case 3S ($C/D = 1.5$, $X_p/R = 3.0$). $Z_{pe}/R = 0.28$ (short); 2.28 (long)

4.5 Effect of Pile Group Positions on Pile Group Settlement and Soil Surface Settlements

To investigate the effect of pile groups on the ground movement, soil surface settlements of cases with and without pile groups are compared at the same locations of potentiometers (P4, P5, and P6) in Fig. 14. Horizontal movements of the pile cap (δx) are also shown in the figure. The settlement increased with increasing the ground loss ratio but showed nonlinearity with the ground loss ratio. At small ground loss ratios ($<4\%$), the settlement rates against $\Delta V/V_0$ was higher than those at relatively large ground loss ratios. Such behaviour was observed in the models without pile groups (Fig. 9). Furthermore, the settlements above the tunnel were relatively larger for the cases with $C/D = 2.5$ than those with $C/D = 1.5$. This difference was more significant at smaller ground loss ratios, which was also seen in Fig. 11.

Compared with the ground surface settlements, the horizontal movements of pile caps are more significantly affected by the test conditions. For the models with pile groups closer to the tunnel ($X_p/R = 2.0$: Case 1D, 4D and 1S), the horizontal movements of pile caps are much greater than those for the cases with $X_p/R = 3.0$ (Case 3D, 6D and 3S).

Short and long piles group with $X_p/R = 2.0$, the case with large vertical load (Case 1D, Fig. 14a), showed large horizontal movements when compared with small vertical loads (Case 4D, Fig. 14c). However, the effect of vertical load became small as pile groups were further from the tunnel ($X_p/R = 3.0$, Fig. 14b, d). The horizontal movements of pile caps with the pile toe depth below the tunnel centre ($Z_{pe}/R = 2.28$, long piles in Case 1S and 3S) were significant reduced (see also Fig. 14e, f). The reduction of pile cap movement may come from the pile groups resting outside the large soil movement zone in



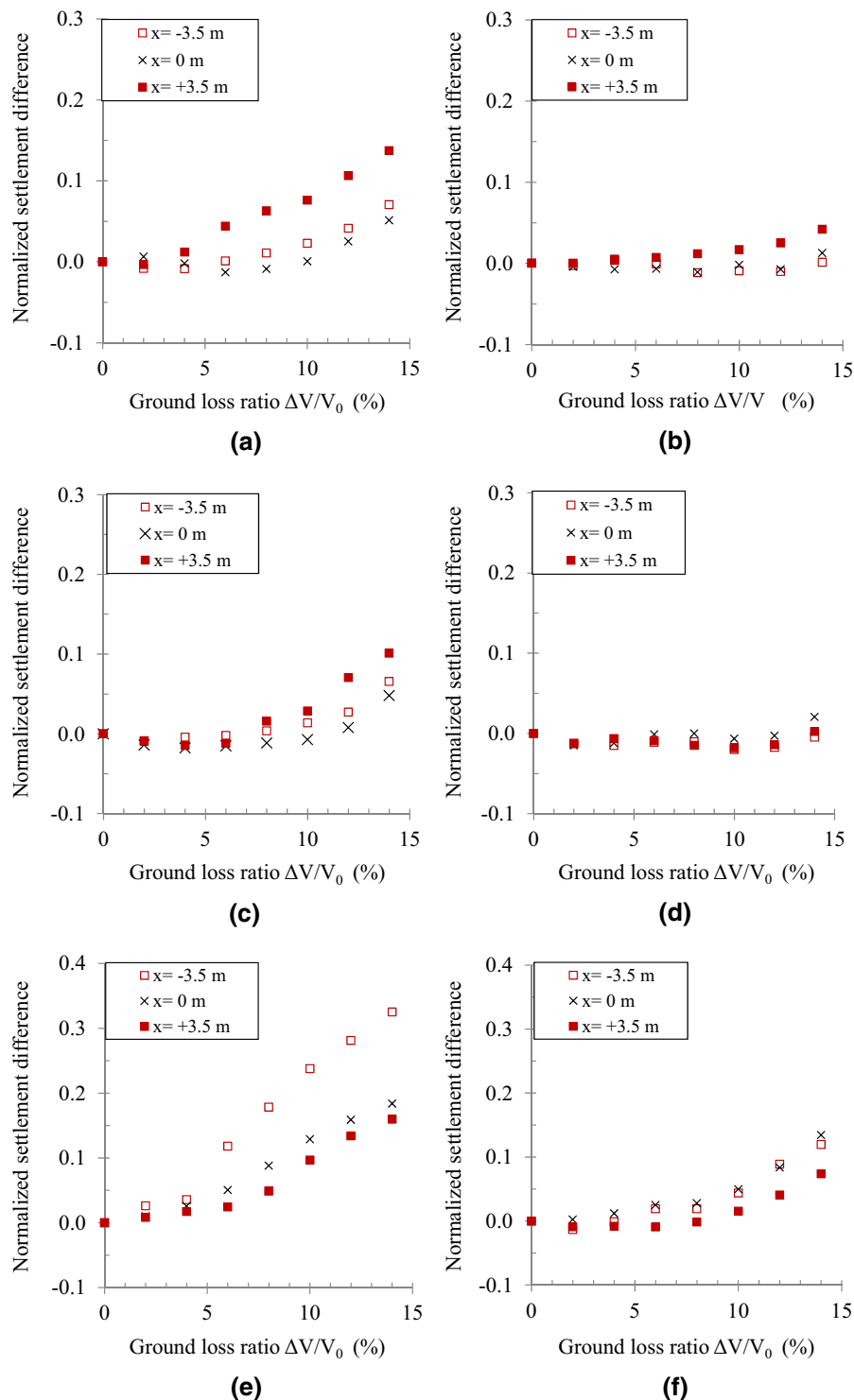


Fig. 15 Difference of ground surface settlement between the cases with and without pile groups: potentiometer measurements. **a** Case 1D ($C/D = 2.5$, $X_p/R = 2.0$). $Z_{pe}/R = -1.72$ (short); 0.28 (long). **b** Case 3D ($C/D = 2.5$, $X_p/R = 3.0$). $Z_{pe}/R = -1.72$ (short); 0.28 (long). **c** Case 4D ($C/D = 2.5$, $X_p/R = 2.0$). $Z_{pe}/$

$R = -1.72$ (short); 0.28 (long). **d** Case 6D ($C/D = 2.5$, $X_p/R = 3.0$). $Z_{pe}/R = -1.72$ (short); 0.28 (long). **e** Case 1S ($C/D = 1.5$, $X_p/R = 2.0$). $Z_{pe}/R = 0.28$ (short); 2.28 (long). **f** Case 3S ($C/D = 1.5$, $X_p/R = 3.0$). $Z_{pe}/R = 0.28$ (short); 2.28 (long)

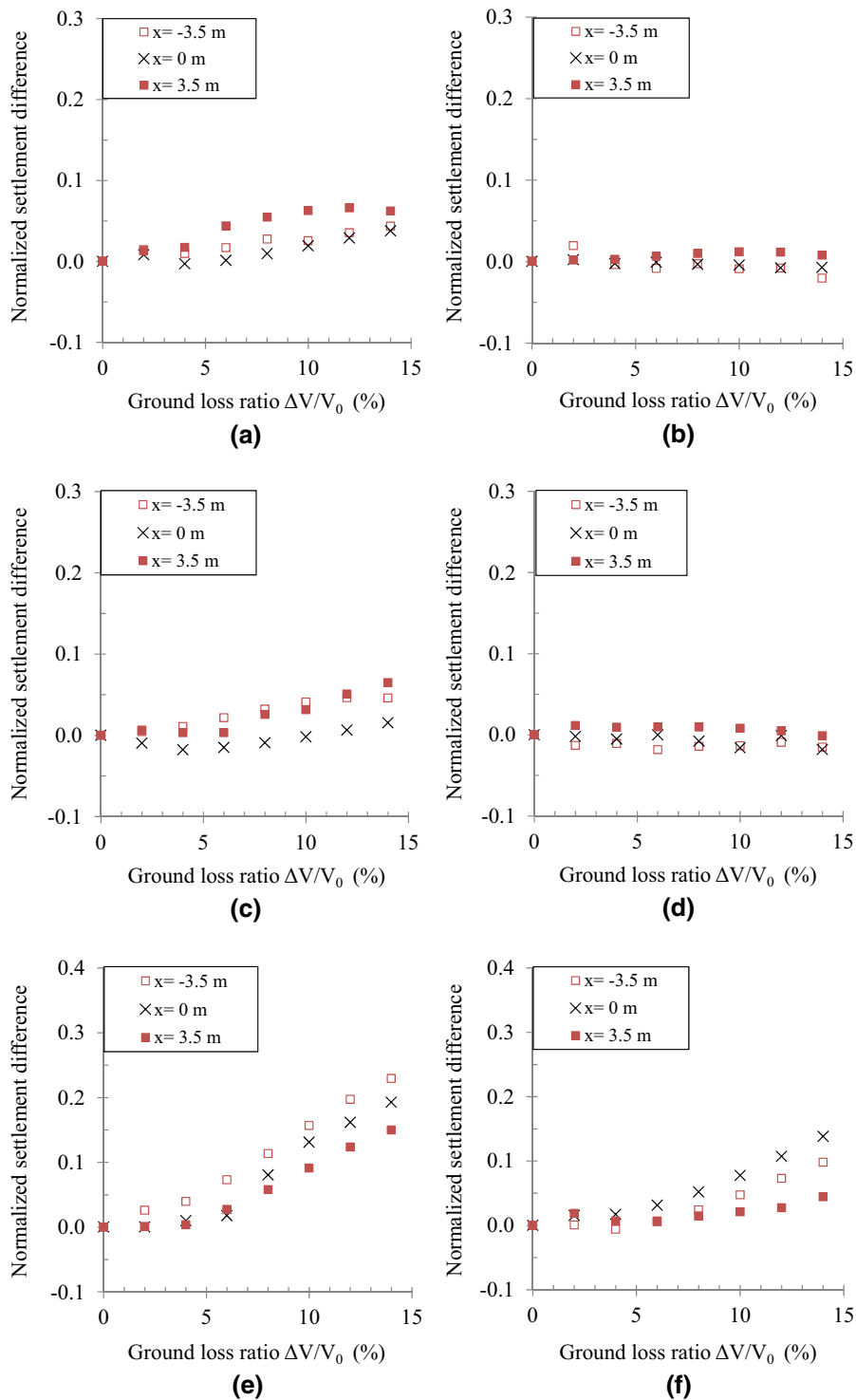


Fig. 16 Difference of ground surface settlement between the cases with and without pile groups: PIV measurements. **a** Case 1D ($C/D = 2.5, X_p/R = 2.0$). $Z_{pe}/R = -1.72$ (short); 0.28 (long). **b** Case 3D ($C/D = 2.5, X_p/R = 3.0$). $Z_{pe}/R = -1.72$ (short); 0.28 (long). **c** Case 4D ($C/D = 2.5, X_p/R = 2.0$). $Z_{pe}/$

$R = -1.72$ (short); 0.28 (long). **d** Case 6D ($C/D = 2.5, X_p/R = 3.0$). $Z_{pe}/R = -1.72$ (short); 0.28 (long). **e** Case 1S ($C/D = 1.5, X_p/R = 2.0$). $Z_{pe}/R = 0.28$ (short); 2.28 (long). **f** Case 3S ($C/D = 1.5, X_p/R = 3.0$). $Z_{pe}/R = 0.28$ (short); 2.28 (long)

the zone of influence proposed by Jacobsz et al. (2004).

Ground movements of the model without pile groups can be considered as a reference in the discussion of the effects of piles on the ground movement due to tunnelling. The differences in the surface settlement between cases with and without pile groups are compared for the potentiometers measurements and PIV in Figs. 15 and 16 respectively. In the figures, normalized settlement difference obtained by Eq. (5) was plotted against the ground loss ratio:

$$\frac{S_p - S_{np}}{S_{np,max}} \quad (5)$$

where S_p is soil surface settlements of cases with pile groups, S_{np} is soil surface settlements of cases without pile groups and $S_{np,max}$ is maximum soil surface settlements of cases without pile groups, that is, the settlement at the tunnel centreline.

As shown in the results of the cases with $C/D = 2.5$ (Fig. 15a–d), the PTM measured settlements of cases 1D and 4D ($X_p/R = 2$) and Case 3D and 6D ($X_p/R = 3$) showed small differences from those of case 0D without a pile group at relatively small ground loss ratios ($<4\% \Delta V/V_0$). However, for the large ground loss ratios ($>4\% \Delta V/V_0$), Case 1D and 3D induced larger vertical settlements than Cases 4D and 6D, especially at the right side of the model ($x = +3.5$ m) in comparison with Case 0D. The reason might come from the presence of the pile group tending to cause a reduction in horizontal compressive strain and hence a reduction in the vertical extension strain in the area above the tunnel crown (Marshall and Mair 2011). As a result, soil settlement propagation due to tunnelling may be increased in the area above the tunnel crown. Additional soil surface settlement in the area of the pile groups were also observed by Lee et al. (2006).

In addition, the presence of pile groups had more effect on induced ground settlements for the cases with $C/D = 1.5$. Case 1S with $X_p/R = 2$ displayed larger settlements at the central part than the case without pile groups (Case 0S), especially at large ground loss ratios ($>4\% \Delta V/V_0$) (Fig. 15e). Ground settlements at the side of short pile groups showed large normalized settlement differences. The influence of pile groups on the surface settlements became less when the pile groups were located far from the tunnel ($X_p/R = 3$) in Fig. 15f. It can be assumed that the pile groups showed more stability

(see also Fig. 14e, f) due to the pile toe resting outside the zone of influence of large soil settlement (Jacobsz et al. 2004). Consequently, the pile groups are behaved like a rigid body and the vertical extension strain is more reduced than the case with $C/D = 2.5$. These mechanisms may explain the reason why differences in soil settlement with $C/D = 1.5$ (Fig. 15e, f) were larger than the cases with $C/D = 2.5$ (Fig. 15a–d).

The trends in settlement differences between cases with and without the pile groups observed by PIV shown in Fig. 16 are similar to those measured by potentiometers (Fig. 15). However, the magnitudes of the differences measured by PIV were smaller than those measured by potentiometers. A possible reason may come from the difference in the location of the measurements between the two methods. Pile groups were installed at the centre line of the container along with the row of potentiometers. On the other hand, the PIV technique measured the ground movements at the container front, which was located at a distance of 5 times the pile diameter from the closest piles in the longitudinal tunnel direction. From the settlement observations at different relative locations of the pile group, it can be said that the effect of existing pile groups was gradually reduced with distance from the pile group. However, there was a certain effect from the pile groups on the ground movement at locations of more than five times the pile diameter, even for the simple pile groups with four piles.

It should be noted that flexible model piles may show smaller pile–soil interaction than the rigid model piles (Marshall et al. 2010), but the effects of the presence of pile groups on settlement of the surrounding soil could still be observed in this study.

5 Conclusions

In this study, a series of centrifuge model tests was conducted on the interaction between dry sand and pile groups using a mechanical two dimensional tunnelling simulator which could introduce a co-axial tunnel diameter reduction imposing from small to large ground losses. The following conclusions were drawn from the study on the effects of pile groups on ground movements.

- From PIV results, it was confirmed that the settlement profiles could be represented by the

Gaussian distribution curve at small and large ground loss ratios. The widths of settlement troughs (x_i values) decreased almost linearly with soil depth. In addition, the presence of pile groups tended to increase the trough width as the pile group position became closer to the tunnel.

- For cases without pile groups, surface settlements measured by PIV at the front of the model showed good agreement with those measured by the PTM at the central cross section axis of the model. This verifies the applicability of PIV for measuring the subsurface displacements. In addition, at large ground loss ratios there are some differences in the observed settlements between the two methods due to the effect of side wall friction, although the magnitude of the difference was small.
- The observed depth variations of the settlement trough width parameter (x_i) showed good agreement with an empirical relation derived from real field sandy soils at small ground loss ratios. The x_i values decreased with increasing ground loss ratio, implying the validity of the tunneling method used in this study.
- Displacements of the pile cap and the soil surface settlements showed non-linearity with respect to the ground loss ratio with a higher settlement rate at small ground loss ratios (<4 %). This behavior was also observed in the model without pile groups.
- The pile group induced more soil surface settlement in the area above the tunnel crown. This trend is more significant for cases with small C/D ($= 1.5$) ratios, small horizontal distances between the pile group and the tunnel X_p/R ($= 2.0$) and large ground loss ratios. However, the induced soil settlement is negligible for the cases with $C/D = 2.5$ and small ground loss ratios.
- There was an effect of the pile groups on the ground movement at locations more than five times the pile diameter away from the piles in the longitudinal direction, even for simple pile groups with four piles.

Acknowledgments The authors would like to acknowledge a research grant from the Centre of Urban Earthquake Engineering, Tokyo Institute of Technology for funding the experiments. The authors also appreciate the very kind support from Toyo Corporation by providing the tunnel machine used for this study.

References

- Attewell PB, Farmer IW (1974) Ground deformations resulting from shield tunnelling in London Clay. *Can Geotech J* 11:380–395
- Barratt DA, Tyler RG (1976) Measurements of ground movement and lining behavior on the London Underground at Regent's Park, Report LR 684. Transport and Road Research Laboratory, Crowthorne
- Bezuijen A, Van der Schrier J (1994) The influence of a bore tunnel on pile foundations. *Proc Centrif* 94:681–686
- Celestino TB, Gomes RAMP, Bortolucci AA (2000) Errors in ground distortions due to settlement trough adjustment. *Tunn Undergr Space Technol* 15(1):97–100
- Cording EJ (1991) Control of ground movements around tunnels in soil. In: *Proceedings of 9th Pan-American conference, soil mechanics and foundation engineering*, Valparaiso, pp 2195–2244
- Dyer MR, Hutchinson MT, Evans N (1996) Sudden valley sewer: a case history. In: Mair R, Taylor R (eds) *Proceeding of international symposium geotechnical aspects of underground construction in soft ground*, Balkema, Rotterdam, The Netherlands, pp 671–676
- Fukushima S, Tatsuoka F (1984) Strength and deformation characteristics of saturated sand at extremely low pressures. *J Soils Found* 24(4):30–48
- Glossop NH (1978) Soil deformation caused by soft ground tunnelling, PhD thesis, Cambridge University
- Hergarden HJAM, Van der Poel JT, van der Schrier JS (1996) Ground movements due to tunnelling: influence on pile foundations. In: Mair R, Taylor R (eds) *Geotechnical aspects of underground construction in soft ground*, Balkema, Rotterdam, pp 519–524
- Imamura S, Nomoto T, Mito K, Ueno K, Kusakabe O (1996) Design and development of underground construction equipment in a centrifuge. In: *Proceeding of international symposium geotechnical aspects of underground construction in soft ground*, London, pp 567–572
- Jacobsz SW (2002) The effects of tunnelling on piled foundation, PhD thesis, University of Cambridge
- Jacobsz SW, Standing JR, Mair RJ, Hagiwara T, Sugiyama T (2004) Centrifuge modelling of tunnelling near driven piles. *J Soils Found* 44(1):49–56
- Kaalberg FJ, Lengkeek HJ, Teunissen EAH (1999) Evaluatie van de meetresultaten van het proefpalenprojek ter plaatse van de tweede Heineenoordtunnel (in Dutch), Adviesbureau Noord/Zuidlijn Report no. R981382, Amsterdam
- Katoh Y, Miyake M, Wada M (1998) Ground deformation around shield tunnel. In: *Proceedings of centrifuge 98*, vol 1, pp 733–738
- König D (1998) An inflight excavator to model a tunneling process. In: *Proceedings of centrifuge 98*, vol 1, pp 707–712
- Lee CJ, Chiang KH (2007) Responses of single piles to tunneling-induced soil movements in sandy ground. *Can Geotech J* 44(10):1224–1241
- Lee CJ, Chen PS, Chiang HT, Chen KF, Lin WL (2006) Evolution of arching effect during tunnelling in sandy soil. In: Ng CWW, Zhang L, Wang YH (eds) *Physical modelling in*

- geotechnics 6th ICPMG' 06, Taylor and Francis Group, London, pp 1171–1176
- Loganathan N, Poulos HG (1998) Analytical prediction for tunneling-induced ground movements in clays. *J Geotech Geoenviron Eng* 124(9):846–856
- Mair R (1979) Centrifuge modelling of tunnel construction in soft clay, PhD thesis, University of Cambridge, UK
- Mair RJ, Taylor RN (1997) Theme lecture: bored tunneling in the urban environment. In: Proceedings of 14th international conference soil mechanics and foundation engineering, Balkema, Rotterdam, The Netherlands, pp 2352–2385
- Mair RJ, Taylor RN, Bracegirdle A (1993) Subsurface settlement profiles above tunnels in clays. *Geotechnique* 43(2):315–320
- Mair RJ, Taylor RN, Burland JB (1996) Prediction of ground movements and assessment of risk of building damage due to bored tunneling. In: Proceeding of international symposium geotechnical aspects of underground construction in soft ground, London, pp 713–718
- Marshall AM, Mair RJ (2011) Tunneling beneath driven or jacked end-bearing piles in sand. *Can Geotech J* 48:1757–1771
- Marshall AM, Klar A, Mair RJ (2010) Tunneling beneath buried pipes: view of soil strain and its effect on pipeline behaviour. *J Geotech Geoenviron Eng* 136:1664–1672
- Marshall AM, Farrell R, Klar A, Mair RJ (2012) Tunnels in sands—the effect of size, depth, and volume loss on greenfield displacements. *Geotechnique* 62(5):385–399
- Moh ZC, Hwang RN, Ju DH (1996) Ground movements around tunnels in soft ground. In: Mair R, Taylor R (eds) Proceeding of international symposium geotechnical aspects of underground construction in soft ground, Balkema, Rotterdam, The Netherlands, pp 725–730
- Nomoto T, Imamura S, Hagiwara O, Kusakabe O, Fujii N (1999) Shield tunnel construction in a centrifuge. *J Geotech Geoenviron Eng* 125(4):289–300
- O'Reilly MP, New BM (1982) Settlements above tunnels in the United Kingdom—their magnitude and prediction. In: *Tunnelling'82*, IMM, London, pp 173–181
- Peck RB (1969) Deep excavation and tunnelling in soft soil. In: Proceedings of 7th conference of soil mechanics and foundation engineering, Mexico, pp 225–290
- Potts RB (1976) Behaviour of lined and unlined tunnels in sand, PhD Thesis, Engineering Department, Cambridge University
- Schmidt B (1969) Settlements and ground movements associated with tunneling in soil, PhD thesis, University of Illinois
- Selemetas D, Standing JR, Mair RJ (2006) The response of full scale piles to tunnelling. In: Geotechnical aspects of underground construction in soft ground, Taylor and Francis Group, London, pp 893–899
- Takemura J, Kimura T, Wong SF (1990) Undrained stability of two dimensional unlined tunnels in soft clay. In: Proceedings of JSCE, No. 418/III-12, pp 267–277
- Takemura J, Kondoh M, Esaki T, Kouda M, Kusakabe O (1999) Centrifuge model tests on double propped wall excavation in soft clay. *Soils Found* 39(3):75–87
- Tatsuoka F, Sakamoto M, Kawamura T, Fukushima S (1986) Strength and deformation characteristics of sand in plane strain compression at extremely low pressures. *Soils Found* 26(1):65–84
- Terzaghi K (1942) *Theoretical soil mechanics*. Wiley, New York
- Vorster TEB (2005) The effects of tunnelling on buried pipes, PhD Thesis, Engineering Department, Cambridge University
- Vorster TEB, Klar A, Soga K, Mair RJ (2005) Estimating the effects of tunnelling on existing pipelines. *J Geotech Geoenviron Eng* 131(11):1399–1410
- White DJ, Take WA (2003) *GeoPIV*, 7.6 eds, Cambridge University Engineering Department
- White DJ, Take WA, Bolton MD (2003) Soil deformation measurement using particle image velocimetry (PIV) and photogrammetry. *Geotechnique* 53(7):619–631